Water Resources Management (2019) 33:337–354
https://doi.org/10.1007/s11269-018-2105-3

Hierarchical Flood Operation Rules Optimization Using Multi-Objective Cultured Evolutionary Algorithm Based on Decomposition

Yongqi Liu[1] · Hui Qin[1] · Li Mo[1] · Yongqiang Wang[2] · Duan Chen[2] · Shusen Pang[3] · Xingli Yin[1]

Received: 5 December 2017 / Accepted: 9 September 2018 /
Published online: 17 September 2018

Abstract

The operation of a reservoir system for flood resources utilization is a complex problem as it involves many variables, a large number of constraints and multiple objectives. In this paper, a new algorithm named multi-objective cultured evolutionary algorithm based on decomposition (MOCEA/D) is proposed for optimizing the hierarchical flood operation rules (HFORs) with four objectives: upstream flood control, downstream flood control, power generation and navigation. The performance of MOCEA/D is validated through some well-known benchmark problems. On achieving satisfactory performance, MOCEA/D is applied to a case study of HFORs optimization for Three Gorges Project (TGP). The experimental results show that MOCEA/D obtains a uniform non-dominated schemes set. The optimized HFORs can improve the power generation and navigation rate as much as possible under the premise of ensuring flood control safety for small and medium floods (smaller than 1% frequency flood). The obtained results show that MOCEA/D can be a viable alternative for generating multi-objective HFORs for water resources planning and management.

Keywords Operation rules · Flood resources utilization · Multi-objective optimization · Decomposition approach · Cultural algorithm

✉ Hui Qin
hqin@hust.edu.cn

[1] School of Hydropower and Information Engineering, Huazhong University of Science and Technology, Wuhan 430074 Hubei, China

[2] Changjiang River Scientific Research Institute, Wuhan, Hubei, China

[3] Three Gorges Cascade Dispatch and Communication Center, Yichang, Hubei, China

1 Introduction

The operation of a reservoir system is generally complex as it involves many variables, a large number of constraints and multiple objectives (Qin et al. 2010). Although simulation models and optimization tools can be used to derive the detailed release policies for each time step of reservoir system (Yeh 1985), a more desirable approach for real-time operation is to optimize operation rules (Karamouz and Houck 1982; Chen et al. 2007). The operation rules can be presented in the form of graphs or tables and define the desired reservoir release or output during each period as a function of water levels, the time of year and inflows. Therefore, giving an optimization operational rule can provide a more practical and reliable guidance to reservoir system operators in the current period. There are two main ways to get such operational rules. One way is to generate optimal input-output patterns by running optimization model first and then extract the release rules using data mining methods (Wei and Hsu 2009; Zhang et al. 2015). Another way is to optimize the rule curves or rule tables directly by optimization algorithm within the constraints (Zhou et al. 2015). This paper focuses on the second way.

Flood disaster is one of the most damaging natural disasters and it usually causes a large amount of economic losses (Cutter et al. 2015). New tactics are needed to help boost flood control. Flood control models have been developed over the past several decades (Marien et al. 1994; Needham et al. 2000; Jia et al. 2016). In addition to flood control requirement, many investigators consider water conservation purposes like hydropower generation and water supply during flood season (Ding et al. 2015). These objectives are often conflict with flood control objective, since flood control requires a certain amount of empty storage for minifying the flood peaks while water conservation requires more remaining storage for hydropower generation or water supply purpose. The problems with multiple conflicting objectives is called multi-objective optimization problems (MOPs). During the past decades, various multi-objective evolutionary algorithms (MOEAs) based on Pareto dominance have been proposed like Multi-objective Genetic Algorithm (MOGA) (Fonseca and Fleming 1993), the Improved Strength Pareto Evolutionary Algorithm (SPEA2) (Zitzler et al. 2001), Nondominated Sorting Genetic Algorithm II (NSGA-II) (Deb et al. 2002), Multi-objective Particle Swarm Optimization (MOPSO) (Coello and Becerra 2004) and Multi-objective Evolutionary Algorithm based on Decomposition (MOEA/D) (Zhang and Li 2007). With the development of MOEAs, more and more researchers have begun to apply MOEAs in multipurpose reservoir operation problems and get good achievements (Reddy and Kumar 2006; Baltar and Fontane 2008; Qin et al. 2010).

In this paper, a multi-objective cultured evolutionary evolution based on decomposition (MOCEA/D) is proposed to optimizing the hierarchical flood operation rules (HFORs) with 4 objectives during flood season. Major contributions are outlined as follows:

1) The HFORs is proposed for flood resources utilization, which mainly focus on small and medium floods. Different HFORs trend to different tradeoffs of flood control objectives and water conservation objectives.
2) A mathematical model with 4 objectives is formulated, which contains upstream flood control objective, downstream flood control objective, power generation objective and navigation objective.
3) A new MOEA named MOCEA/D is proposed. The algorithm combines the advantages of Cultural Algorithm (CA) (Reynolds 1994) and MOEA/D and shows its high performance when solve some well-known test functions.

4) MOCEA/D is applied to solve the multi-objective HFORs optimization problem: a case study of Three Gorges Project (TGP).

The rest of the paper is organized as follows: section 2 introduces the HFORs and formulates the multi-objective mathematical model. Section 3 describes MOCEA/D in detail. Section 4 applies MOCEA/D to a practical HFORs optimization problem and analyzes the experimental results. Section 5 concludes this work.

2 HFORs and Mathematical Model

This section first introduces the general form of HFORs, then formulates the mathematical model with multi-objectives and several constraints.

2.1 HFORs

The operational rules are usually presented in the form of graphs or tables, define the desired reservoir release as a function of existing storage volumes, the date time of year, and inflows. In HFORs, water level and expected inflow are taken into consideration for then function. The water level and inflow can be divided into different interval $Z_i \in [Z_i^l, Z_i^u]$, $I_j \in [I_j^l, I_j^u]$, Z_i and I_j denote the i-th hierarchical water level and j-th hierarchical inflow, l and u represent the lower and upper bound of the interval. The general HFORs can be express as a function as follow:

$$R_{ij} = f\left(Z_i, I_j\right) \tag{1}$$

Where R_{ij} is the desired reservoir release under the i-th hierarchical water level and j-th hierarchical inflow.

2.2 Objective Function

The target of this study is to obtain optimal HFORs for regulating small and medium floods, in which many objectives and constraints should be considered. The objectives are expressed as follows:

Flood control objectives: generally, there are two goals for reservoir flood control: reducing flood disaster in the downstream flood protection area and flood control requirement for reservoir area. Considering these two goals, the two objectives of flood control are expressed as follows.

$$\min F_1 = \min_{\forall t=1,2,\ldots,T} \{\max(Z_t)\} \tag{2}$$

$$\min F_2 = \min_{\forall t=1,2,\ldots,T} \{\max(R_t)\} \tag{3}$$

Where T is the number of periods; R_t is the discharge volume of the t-th period; Z_t is the upstream water level of the reservoir during the t-th period.

Maximizing hydropower generation of the reservoir system:

$$\max F_3 = \sum_{t=1}^{T} N_t \Delta t = \sum_{t=1}^{T} A H_t q_t \Delta t \tag{4}$$

Where N_t is power output of the t-th period; Δt is the operation interval; A is the power production coefficient of the hydropower plant; H_t is net head of the t-th period and q_t is the release passing turbines of the t-th period.

Maximum guarantee rate of navigation:

$$\max F_4 = \frac{1}{T} \sum_{t=1}^{T} f_n(R_t) \tag{5}$$

Where $f_n()$ is the function of navigation guarantee rate, which is related to discharge volume R_t.

2.3 Constraints

The optimization is subject to the following constraints:

(1) Water balance constraint:

$$S_t = S_{t-1} + I_t - R_t \tag{6}$$

Where S_t is the reservoir storage of the t-th period; I_t and Q_t are the reservoir inflow and discharge volume during t-th period, respectively.

(2) Water level constraint:

$$Z_t^{\min} \le Z_t \le Z_t^{\max} \tag{7}$$

Where $Z_t^{\min}$ is minimum limit of upstream water level during the t-th period, $Z_t^{\max}$ is the maximum limit of upstream water level during the t-th period.

(3) Water release capacity constraint:

$$R_t \le R_{\max}(Z_t^{avg}) \tag{8}$$

Where Z_t^{avg} is the average upstream water level of the t-th period, $R_{\max}(Z_t^{avg})$ is the release ability function of Z_t^{avg}.

(4) Discharge volume constraint:

$$R_t^{\min} \le R_t \le R_t^{\max}, t \in [1, T] \tag{9}$$

Where R_t^{min} and R_t^{max} are the minimum and maximum limit of discharge volume during the *t*-th period..

(5) Power-generation limits:

$$N_t^{min} \le N_t \le N_t^{max} \tag{10}$$

Where N_t^{min} and N_t^{max} are the minimum and maximum limit of power output during the *t*-th period.

3 Multi-Objective Cultured Evolutionary Algorithm Based on Decomposition

In this section, the MOCEA/D is described in detail, which incorporate the advantages of CA and MOEA/D. Firstly, some basic concepts related to MOEA/D and CA are provided, then the major procedures of MOCEA/D are described in detail, at last it performance is verified by using some benchmark test problems.

3.1 Background

3.1.1 Deposition for Multi-Objective Optimization

MOEA/D requires a decomposition approach for converting approximation of a MOP into a number of single objective optimization problems. The 3 most commonly used decomposition approaches are weighted sum, weighted Tchebycheff, and boundary intersection approaches. In this paper, we use the penalty-based boundary intersection (PBI) approach. The *i*-th subproblem is defined as:

$$\text{minimize}\, g^{pbi}\left(x|\lambda^i, z^*\right) = d_1^i + \theta d_2^i \tag{11}$$

subject to $x \in \Omega$.

Where:

$$d_1^i = \|\left(F(x) - z^*\right)^T \lambda^i\| / \|\lambda^i\| \tag{12}$$

$$d_2^i = \|F(x) - z^* - \left(d_1^i / \|\lambda^i\|\right) \lambda^i\| \tag{13}$$

$\lambda^i = \left(\lambda_1^i, \ldots, \lambda_m^i\right)^T$ is a weight vector for the *i*-th subproblem, i.e.,$\lambda_j^i \ge 0$ for all$j = 1, \ldots, m$and$\sum_{j=1}^m \lambda_j^i = 1$; $z^* = \left(z_1^*, \ldots, z_m^*\right)^T$is the reference point, i.e., $z_i^* = \min\{f_i(x)|x \in \Omega\}$for each $i = 1, \ldots, m$; Ω is the decision space; θ (>0) is a preset penalty parameter; $\|\cdot\|$ denotes the Euclidean distance.

3.1.2 Cultural Algorithm

CA is a technique that add domain knowledge to improve the performance of evolutionary algorithms (Renfrew 1994). The main features of CA are population space and belief space. Population space consists of a set of individuals, which will be updated according to some evolutionary algorithms (Reynolds 1994; Landa Becerra and Coello 2006). Belief space contains different kinds of knowledge, which can be learned from the evolutionary process. After that, the knowledge will be used to guide the evolutionary process in population space. The key technology of CA is how to define the knowledge in the belief space and how to guide the operators of the evolutionary algorithm. In this paper, we define two knowledge structures and use MOEA/D as the population space of CA.

3.2 Proposed Algorithm: MOCEA/D

3.2.1 Framework of MOCEA/D

The framework of MOCEA/D is presented in Algorithm 1. First, the weight vectors are generated by (Das and Dennis 1998) systematic approach. Then, the neighborhood index set, population, archive set, and the evolutionary parameters of MOCEA/D are initialized by initialization procedure. In the main while-loop, for each subproblem, a new offspring is generated according to the reproduction procedure. After reproduction, the parent solution and evolutionary parameters will be updated according to the comparison mechanisms in step 11. Finally, the belief space is updated following the new population space. In the following sections, the major procedures of RSEA are described in detail.

Algorithm 1 Framework of the RSEA

1 $(\boldsymbol{\lambda}^1, \boldsymbol{\lambda}^2, \ldots, \boldsymbol{\lambda}^N)$ = InitializeWeights()
2 E = InitializeNeighborhood() // E is the neighborhood index set
3 P = InitializePopulation() // P is the population in population space
4 $\mathbf{z}^*$ = InitializeIdealPoint(P)
5 *arcS*, **F**, **CR** = InitializeBeliefSpace(P) // *arcS* is the archive set, **F** and **CR** are evolutionary parameters in belief space
6 **while** *termination criteria is not satisfied* **do**
7   **for** *each subproblem i = 1, 2, . . . , N* **do**
        // determine the mating/update pool
8   Set $MP = \begin{cases} P(E_i) & rnd < \delta \\ arcS & \text{otherwise} \end{cases}$
9         $\mathbf{x}^c$, F, CR = Reproduction(MP, F_i, CR_i) // $\mathbf{x}^c$ is an offspring
10         $\mathbf{z}^*$ = UpdateIdealPoint($\mathbf{x}^c$)
11   P, **F**, **CR** = UpdtaePopulation(MP, $\mathbf{x}^c$, F, CR)
12   **end for**
13   *arcS* = TruncationOperation (P, *arcS*)
14 **end while**

3.2.2 Belief Space

Two kinds of knowledge is proposed in MOCEA/D: situational knowledge and normative knowledge.

1) Situational knowledge: it consists of a series of non-inferior solutions named archive set, which represent the best solutions obtained from the population space. After the evolution of each generation, it need to find all non-dominated individuals from this generation and add them into situational knowledge. Then, a truncation operation is applied to reduce archive set if its size exceeds N_Q, N_Q is the predefined size of archive set. The truncation operator we employ is similar with the truncation operator in SPEA2, which sort the solutions by the distance to the k-th nearest data point (Zitzler et al. 2001)

This situational knowledge can influence the mating and update pool of MOCEA/D in Algorithm 1, step 8. On the one hand, the Archive set contains the best elites of the entire evolutionary which can give more useful information for reproduction procedure. On the other hand, the situational knowledge has its own truncation operator, which can maintain the diversity of the archive set. Therefore, the offspring will have a low probability of falling into local optimum.

2) Normative knowledge: it consists of N groups of evolutionary algorithm parameters, N is equal to the size of population. In this paper, MOCEA/D use DE as the evolutionary algorithm, which contains parameters F and CR. To choose suitable parameters adaptively, we use the belief space to dynamically update the parameters to improve the performance of the algorithm.

First, all parameters **F** and **CR** are set randomly within a reasonable range, each set of parameters F_i and CR_i corresponds to subproblem i. Before the DE operator of the i-th subproblem, new parameters are generated as follow

$$F = \begin{cases} F_{\min} + rand_1()\cdot(F_{\max} - F_{\min}) & rand_2() < \tau_1 \\ F_i & otherwise \end{cases} \tag{14}$$

$$CR = \begin{cases} CR_{\min} + rand_3()\cdot(CR_{\max} - CR_{\min}) & rand_4() < \tau_2 \\ CR_i & otherwise \end{cases} \tag{15}$$

Where $rand_{1-4}()$ are four mutually independent random numbers between 0 and 1. $F_{\min}$ and $F_{\max}$ are the minimum and maximum values of F. $CR_{\min}$ and $CR_{\max}$ are the minimum and maximum values of CR. τ_1 and τ_2 are the threshold values between 0 and 1. According to our experiment, $F_{\min}$ and $F_{\max}$ are set as 0 and 1, $CR_{\min}$ and $CR_{\max}$ are set as 0 and 1, $\tau_1 = \tau_2 = 0.01$.

Then, the offspring solution $\mathbf{x}^c$ is generated by a classic DE (DE/rand/1/bin) (Storn and Price 1997) with the new parameters F and CR. And the parameter of k-th subproblem F_k and CR_k will be updated as F and CR follow the offspring, in Algorithm 2 step 6 and step 10.

3.2.3 Update Procedure and Constraint Handling

In the original MOEA/D, the comparison of two solutions is entirely based on the decomposition approach like PBI. This single way of evaluation may loss some elite during the evolutionary process. MOCEA/D combines dominance relations with PBI approach to improve the update procedure. When the offspring $\mathbf{x}^c$ is compared with parent solution $\mathbf{p}$, the dominance relations of the two solutions is measured first. If $\mathbf{x}^c$

dominate **p**, then the solution **p** is replaced by the offspring $\mathbf{x}^c$; otherwise, the solution **p** is kept; if neither of them is dominated by the each other, then we compare them according to the PBI value.

As for constrained problems, a simple scheme is used, which modify the definition of domination between two solutions i and j. After checking their constraints, if 1) solution i is feasible and solution j is not, 2) solutions i and j are both infeasible, but solution i has a smaller overall constrains violation, 3) solutions i and j are feasible and solution i dominates j, it said that solution i is constrained-dominate the solution j. The update procedure is presented in Algorithm 2.

Algorithm 2 UpdtaePopulation(MP, $\mathbf{x}^c$, F, CR)

Set $c = 0$.
while $c < 1$ and $MP \neq \emptyset$ **do**
    Randomly pick an index j from MP
    $MP := MP \setminus \{j\}$
    if $\mathbf{x}^c$ constrained-dominate $\mathbf{p}^j$ **then**
        $\mathbf{p}^j = \mathbf{x}^c$, $F_j = F$, $CR_j = Cr$
        $c = c+1$;
    else if $\mathbf{p}^j$ don't constrained-dominate $\mathbf{x}^c$ **then**
        if $g(\mathbf{x}^c \mid \lambda^j, z^*) \leq g(\mathbf{p}^j \mid \lambda^j, z^*)$ **then**
            $\mathbf{p}^j = \mathbf{x}^c$, $F_j = F$, $CR_j = Cr$
            $c = c+1$
        end
    end
end

3.3 Test Suites and Experimental Results

3.3.1 Benchmark Problems and Performance Metrics

To demonstrate the performance of MOCEA/D, DTLZ1 to DTLZ4 (Deb et al. 2005) are used for our experimental studies. The number of objectives for each benchmark problem are varies from 3 to 8. As recommended in reference (Deb and Jain 2014), the number of variables are $(m + k - 1)$, where m is the number of objectives and $k = 5$ for DTLZ1, while $k = 10$ for DTLZ2, DTLZ3, and DTLZ4.

To measure both the convergence and diversity of the Pareto-optimal set, the inverse generational distance (IGD) metric (Deb and Jain 2014) is used. Let P^* be a set of uniformly distributed points along the Pareto Front (PF). A is the final nondominated solutions set obtained by an algorithm. The IGD value of A is computed as:

$$IGD(A, P^*) = \frac{1}{|P^*|} \sum_{i=1}^{|P^*|} \min_{j=1}^{|A|} d(p_i, a_j) \tag{16}$$

Where $d(p_i, a_j) = \|p_i - a_j\|_2$. The lower value of $IDG(A, P^*)$ means the algorithm obtains a better solutions set A.

3.3.2 Results and Discussion

To verify MOCEA/D, three evolutionary algorithms, including NSGA-III, MOEA/D-SBX, and MOEA/D-DE are considered for comparisons. For each algorithm, 20 independently run is applied on each problem. And the termination is a predefined number of generation for each run, listed in Table 1. The parameter settings for comparisons algorithms NSGA-III, MOEA/D-SBX, and MOEA/D-DE are according to the reference (Deb and Jain 2014). The parameters of MOCEA/D are the same as MOEA/D-DE.

Table 1 presents the best, median and worst IGD values obtained by MOCEA/D, NSGA-III, MOEA/D-SBX and MOEA/D-DE on m-objective DTLZ1–4 problems. As shown in Table 1, MOCEA/D performs slightly better for DTLZ1, DTLZ3 and DTLZ4 than other algorithms. For DTLZ2 problems, the performance of MOEA/D-SBX is better than MOCEA/

Table 1 Best, median and worst IGD values obtained by MOCEA/D, NSGA-III, MOEA/D-SBX and MOEA/D-DE on m-objective DTLZ1–4 problems. Best performance is shown in bold

problem	m	MaxGen	MOCEA/D	NSGA-III	MOEA/D-SBX	MOEA/D-DE
DTLZ1	3	400	5.047E-07	4.880E-04	4.095E-04	5.470E-03
			5.971E-06	1.308E-03	1.495E-03	1.778E-02
			7.301E-05	4.800E-03	4.743E-03	3.394E-01
	5	600	3.305E-06	5.116E-04	3.179E-04	2.149E-02
			4.621E-05	9.799E-04	6.372E-04	2.489E-02
			5.166E-04	1.978E-03	1.635E-03	3.432E-02
	8	750	7.906E-04	2.044E-03	3.914E-03	3.849E-02
			3.592E-03	3.979E-03	6.106E-03	4.145E-02
			6.965E-03	8.721E-03	8.537E-03	4.815E-02
DTLZ2	3	250	1.232E-04	1.262E-03	5.432E-04	3.849E-02
			4.065E-04	1.357E-03	6.406E-04	4.562E-02
			9.038E-04	2.144E-03	8.006E-04	6.069E-02
	5	350	2.689E-03	4.254E-03	1.219E-03	1.595E-01
			4.261E-03	4.982E-03	1.437E-03	1.820E-01
			6.082E-03	5.862E-03	1.727E-03	1.935E-01
	8	500	8.480E-03	1.371E-02	3.097E-03	3.003E-01
			2.726E-02	1.571E-02	3.763E-03	3.194E-01
			4.833E-02	1.811E-02	5.198E-03	3.481E-01
DTLZ3	3	1000	1.690E-05	9.751E-04	9.773E-04	5.610E-02
			7.128E-05	4.007E-03	3.426E-03	1.439E-01
			2.269E-04	6.665E-03	9.113E-03	8.887E-01
	5	1000	2.007E-04	3.086E-03	1.129E-03	1.544E-01
			9.296E-04	5.960E-03	2.213E-03	2.115E-01
			3.726E-03	1.196E-02	6.147E-03	8.152E-01
	8	1000	1.406E-02	1.244E-02	6.459E-03	2.607E-01
			3.084E-02	2.375E-02	1.948E-02	3.321E-01
			5.234E-02	9.649E-02	1.123	3.923
DTLZ4	3	600	1.761E-05	2.915E-04	2.929E-01	3.276E-01
			2.246E-05	5.970E-04	4.280E-01	6.049E-01
			7.776E-05	4.286E-01	5.234E-01	3.468E-01
	5	1000	7.767E-05	9.849E-04	1.080E-01	1.090E-01
			3.083E-04	1.255E-03	5.787E-01	1.479E-01
			1.862E-03	1.721E-03	7.348E-01	4.116E-01
	8	1250	8.465E-04	5.078E-03	5.298E-01	2.333E-01
			4.911E-03	7.054E-03	8.816E-01	3.333E-01
			2.291E-02	6.051E-01	9.723E-01	7.443E-01

*Results of NSGA-III, MOEA/D-SBX and MOEA/D-DE are taken from (Deb and Jain 2014)

D. But the performances of MOCEA/D is better than MOEA/D-DE and are similar to NSGA-III. Figure 1 shows the nondominated solutions obtained by MOCEA/D for the three-objective DTLZ1 to DTLZ4. It can be seen that the solutions are get close to the PF and also get a uniform distribution on the whole PF.

4 Case Study: Multi-Objective HFORs Optimization for TGP

The TGP, with the largest installed hydro power capacity in the world, is located in the Yangtze River. The normal water level is 175 m, the total reservoir storage capacity is 39.3 billion m^3. The flood control limit level is 145 m and the flood control storage capacity is 22.15 billion m^3. Installation capacity and firm power output of it are 22,500 and 4990 MW respectively.

4.1 Flood control indicators

For flood control, TGP have to not only minify the flood peaks for downstream areas but also control the water level for preventing potential major flood and dam safety. Different flood

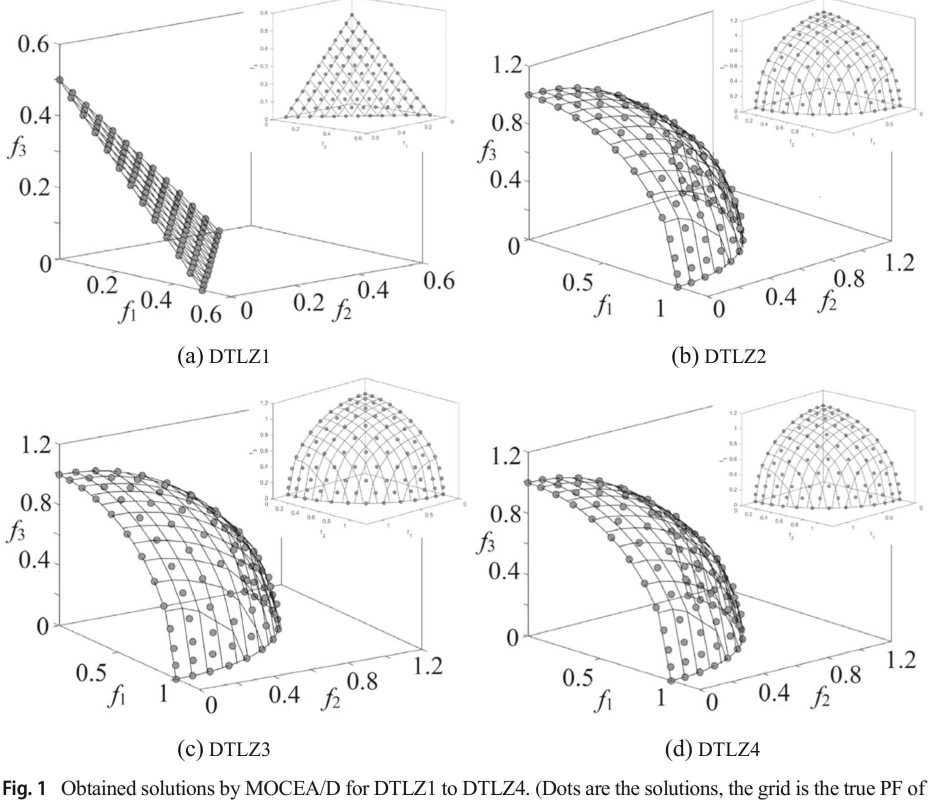

(a) DTLZ1 (b) DTLZ2 (c) DTLZ3 (d) DTLZ4

Fig. 1 Obtained solutions by MOCEA/D for DTLZ1 to DTLZ4. (Dots are the solutions, the grid is the true PF of each problem)

Table 2 The Navigation Standard of TGP

Ship power (kW)	Ascending discharge (m^3/s)	Descending discharge (m^3/s)	Ship power (kW)	Ascending discharge (m^3/s)	Descending discharge (m^3/s)
630 kW or more	45,000	45,000	270 kW to 368 kW	30,000	35,000
440 kW to 630 kW	40,000	45,000	200 kW to 270 kW	25,000	30,000
368 kW to 440 kW	35,000	40,000	200 kW or less	25,000	25,000

control tasks map to different thresholds of discharge value and water level. The flood control indicators with corresponding discharge value and water level are summarize as follow:

1) To keep the flood control limit level, discharge value should equal to inflow, water level should be controlled as 145 m;
2) For the safety of Chenglingji station, discharge value should less than 40,000 m^3/s, water level should under 171 m;
3) For the warning water level of Shashi station (43 m, 44.5 m and 45 m), discharge value should less than 45,000 m^3/s, 55,000 m^3/s, 61,000 m^3/s respectively, water level should under 171 m;
4) To keep the streamflow of Zhicheng station less than 80,000 m^3/s, discharge value should less than 76,000 m^3/s respectively, water level should under 175 m;
5) For dam safety, water level should under 175 m.

4.2 Guarantee rate of navigation

For navigation rule, the ship locks will not allow navigation when the discharge volume of the Three Gorges Reservoir is greater than 45,000 m^3/s. Moreover, when the discharge volume is between 25,000 to 45,000 m^3/s, TGP will restrict the navigation according to the different size of the ships' power. When the discharge volume is between 3200 to 25,000 m^3/s, ships of all sizes can pass through the ship locks. The navigation standard is shown in Table 2.

According to the actual navigable ship classification statistics from 2003 to 2013: ships with power less than 200 kW accounted for 16.49%, 200 ~ 270 kW accounted for 21.60%, 270

Table 3 HFORs table for TGP

Inflow (10^4 m^3/s) Water level (m)	[0, 3)	[3,4)	[4,5)	[5,5.5)	[5.5, +∞)
[145, 146.5)	Inflow	X_1	X_2	X_3	X_4
[146.5, 150)	X_5	X_6	X_7	X_8	X_9
[150, 155)	X_{10}	X_{11}	X_{12}	X_{13}	X_{14}
[155, 160)	X_{15}	X_{16}	X_{17}	X_{18}	X_{19}
[160, 165)	X_{20}	X_{21}	X_{22}	X_{23}	X_{24}
[165, 171)	X_{25}	X_{26}	X_{27}	X_{28}	X_{29}
[171, 175)	Discharge according design rule				
175	Discharge according design rule				

Table 4 Non-dominated operation schemes of HFORs

Index	Max water level (m)	Max discharge (m^3/s)	Power generation (10^8 kWh)	Navigation rate (%)	Index	Max water level (m)	Max discharge (m^3/s)	Power generation (10^8 kWh)	Navigation rate (%)
1	145.8	49,096	533.3	77.8	31	153.0	47,336	567.3	75.4
2	147.0	48,616	534.2	77.8	32	153.1	43,105	558.0	78.8
3	147.1	46,863	534.4	77.6	33	153.3	45,372	561.5	78.4
4	148.1	45,624	535.7	77.3	34	153.4	45,752	566.5	73.9
5	148.1	48,080	537.4	76.7	35	153.6	45,864	565.3	79.2
6	148.3	49,017	540.3	77.2	36	153.8	44,182	567.1	73.7
7	148.9	46,720	536.8	77.9	37	153.9	47,320	570.2	75.0
8	149.4	47,335	539.8	78.6	38	154.0	47,171	570.5	79.6
9	149.4	45,566	539.1	76.7	39	154.1	45,482	570.2	77.7
10	149.6	47,535	548.2	75.5	40	154.5	42,319	560.8	78.6
11	149.6	47,052	544.2	77.2	41	154.7	45,912	574.0	77.0
12	150.4	47,668	548.7	79.6	42	154.8	43,370	568.9	73.8
13	150.4	44,095	540.2	76.9	43	154.9	43,708	567.8	78.0
14	150.5	45,700	544.3	78.8	44	155.0	44,879	572.0	79.4
15	150.5	46,348	546.6	75.7	45	155.3	44,411	572.5	74.4
16	150.6	46,748	552.2	74.5	46	155.5	44,988	576.5	73.6
17	151.0	48,792	557.9	75.5	47	155.6	45,342	575.8	80.1
18	151.3	47,385	556.8	77.7	48	156.0	43,022	572.5	74.7
19	151.3	46,067	554.4	76.0	49	156.0	43,072	571.7	78.5
20	151.4	45,270	549.8	77.8	50	156.3	44,692	578.8	74.7
21	151.4	43,379	542.8	77.5	51	156.4	43,121	578.7	73.5
22	151.5	47,251	560.6	74.7	52	156.7	43,516	576.6	79.6
23	151.7	44,701	551.8	75.1	53	157.2	44,401	582.7	75.1
24	151.7	48,092	562.0	78.7	54	157.3	42,672	581.7	73.0
25	152.0	43,450	551.8	78.6	55	157.3	44,609	581.7	80.2
26	152.0	45,755	557.7	75.7	56	157.6	42,733	578.9	79.4
27	152.1	45,988	561.3	74.3	57	157.9	44,894	585.7	80.1
28	152.2	45,026	556.4	79.2	58	158.0	42,575	582.6	79.5
29	152.4	46,215	561.1	79.2	59	158.6	43,338	587.2	73.2
30	152.7	47,018	564.8	79.5	60	158.8	43,290	588.6	79.5

*The max water level value, discharge volume, power generation and navigation rate are the average values among whole 130 years

~ 368 kW accounted for 26.49%, 368 ~ 440 kW accounted for 16.79%, and 440 ~ 630 kW accounted for 7.19%, 11.46% of the ships with a power of more than 630 kW. Assuming that the proportions of the ascending (passing through the ship locks from downstream to upstream) and descending (passing through the ship locks from upstream to downstream) ships are the same, the mapping relation between the discharge volume of the TGP and the guarantee rate of the navigation can be established.

4.3 HFORs for TGP

According to the general HFORs and flood control indicators for TGP. This section proposes the HFORs for TGP, presented in Table 3. It mainly focus on small and medium floods and ensure the discharge volume of TGP less than 55000m^3/s (upper bound of $X_{1\sim29}$). The water level of TGP must be lower than 171 m for the potential major flood. When the water level is higher than 171 m, TGP should discharge according original designed rules. As is shown in

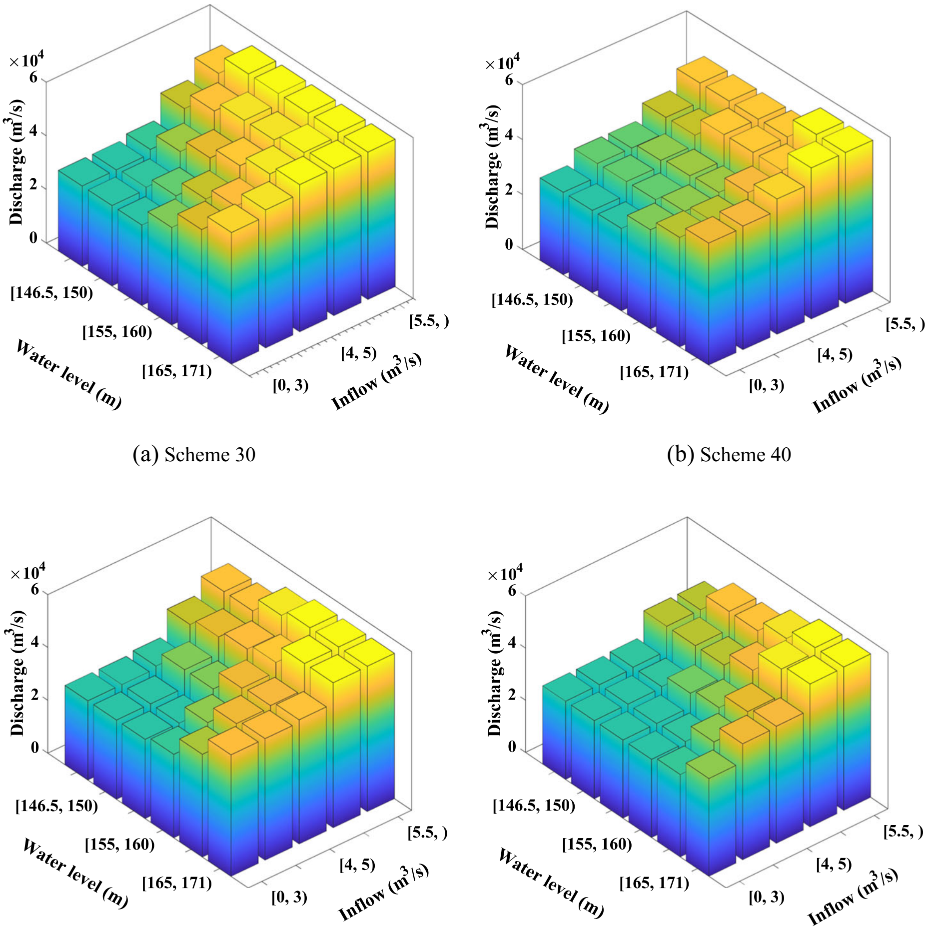

(a) Scheme 30 (b) Scheme 40

(c) Scheme 47 (d) Scheme 60

Fig. 2 The HFORs chart of Scheme 30, 40, 47, 60

Table 3, the decision variables X_1~X_{29} denote discharge volume R_{ij}. The bound of every decision variable is set as [3, 5.5] (10^4 m^3/s). In addition to the constraints expressed in section 2, the HFORs are generated follow the regulation that$\forall j\ R_{ij} \le R_{i+1,j}$, $\forall i\ R_{ij} \le R_{i,j+1}$ and all the decision variables are divisible by 100 m^3/s.

The simulation model of the HFORs is executed according to the following step: (1) Get the current inflow I_t and water level Z_t of TGP. (2) Find the desire discharge volume R_t according to the HFORs. (3) Calculate the water level of next time $Z_{t\text{-}1}$. If $Z_{t\text{-}1}$ is less than the minimum limit of water level or larger than the maximum limit of water level, set $Z_{t\text{-}1}$ as the limit values and update the discharge volume R_t.

4.4 Results and Discussion

MOCEA/D is applied to optimize the HFORs for TGP with four objectives. A total of 130 years (From 1882 to 2011) historical daily streamflow during flood season (From June 11

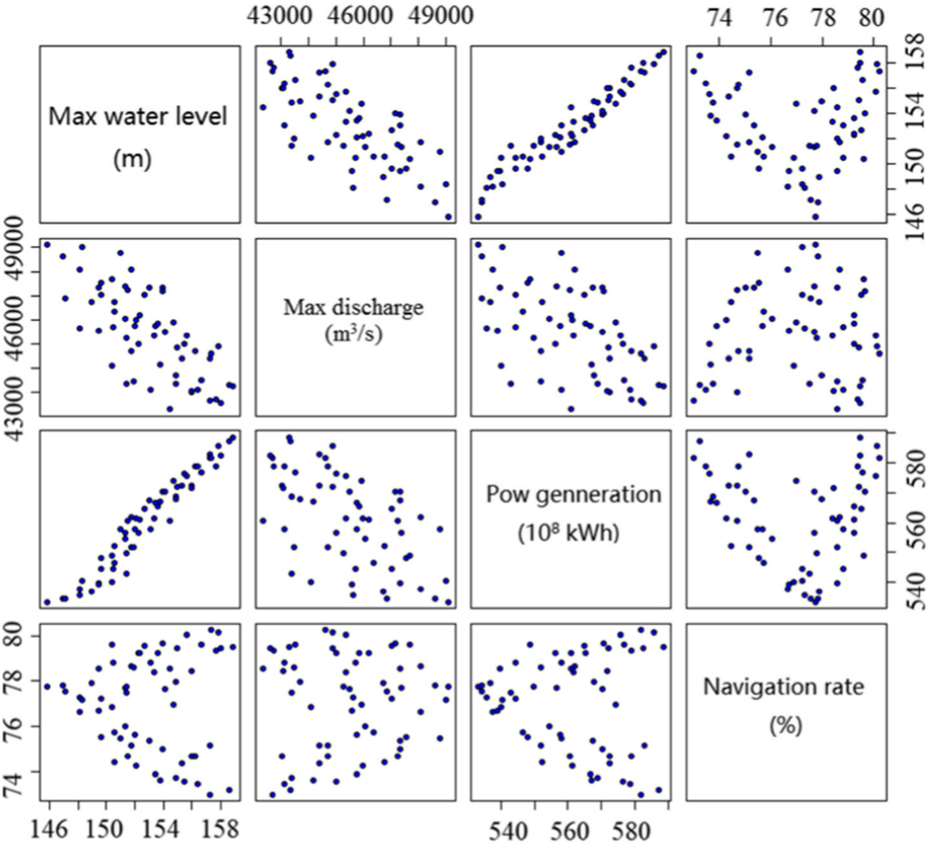

Fig. 3 MOCEA/D solutions are shown using scatterplot matrices of 4 objectives

to October 31, 143 days) of Yichang station is used as inflow of TGP in the simulation. The starting regulation level for every year is 145 m. The population space is composed of $N = 120$ individuals, and the belief space can accommodate up to $N_Q = 60$ individuals, the maximum number of generations *GenNum* is set to 500.

4.4.1 Results of the Application

Tables 4 presents the obtained non-dominated schemes of HFORs for TGP, the 4 objectives of every scheme max water level, max discharge volume, power generation and navigation rate are listed. All solutions satisfy the flood control constraints: maximum water levels are lower than 171 m and maximum discharge volumes are less than 5.5×10^4 m^3/s. From Table 4 we can see that, the average maximum water levels are in the range that from 145.8 (Scheme 1) to 158.8 m (Scheme 60). The average maximum discharge volumes are decreased from 49,096 (Scheme 1) to 42,319 m^3/s (Scheme 40). The average annual power generation are in the range from 533.3 (Scheme 1) to 588.6 (Scheme 60) $\times 10^8$ kWh, which means Scheme 60 can increase the average annual power generation by 10.37%. The average navigation rate can be optimized to 80.2% (Scheme 55), which the average navigation rate of original designed rule is 77.8% (Scheme 1).

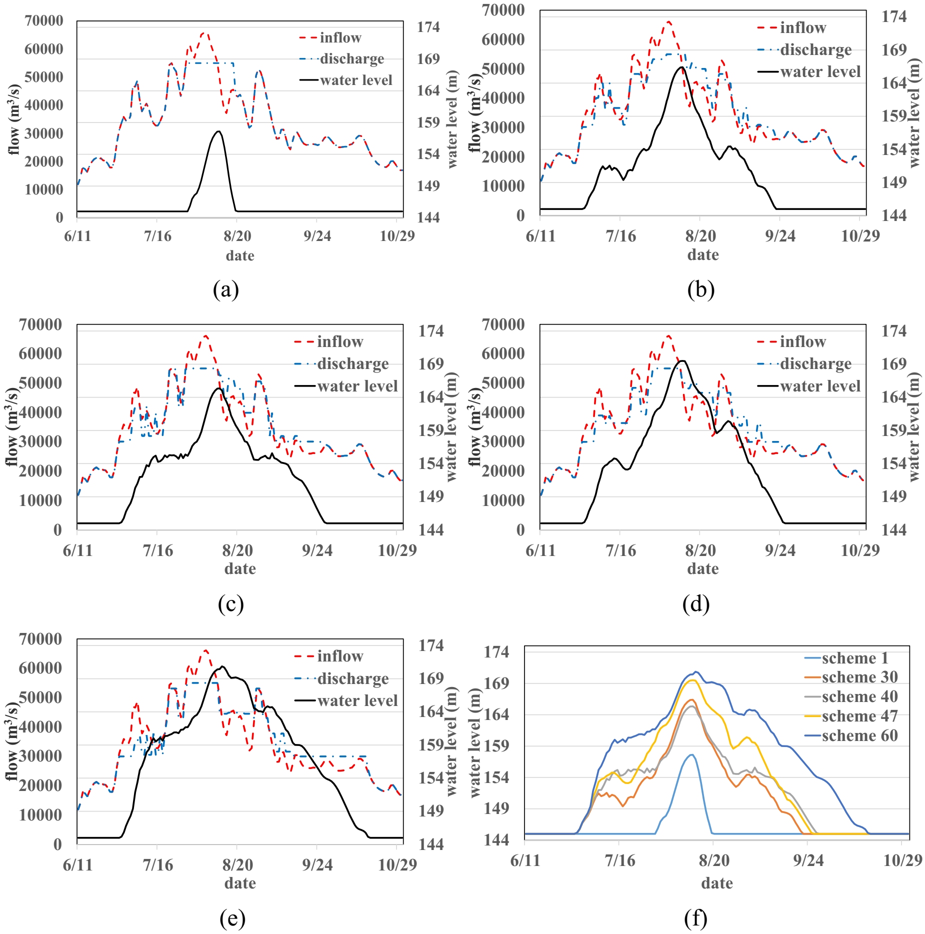

Fig. 4 Discharge processes and water lever processes of **a** Scheme 1, **b** Scheme 30, **c** Scheme 40, **d** Scheme 47, and **e** Scheme 60 for the flood in 1954; **f** water lever process of different schemes for the flood in 1954

The HFORs can be expressed as a three-dimensional chart like Fig. 2. The HFROs chart can visually give the discharge volume values with different water levels and inflows. In the figures, the coordinate axis in X direction stand for different inflow hierarchies, Y direction stand for different water level hierarchies and Z direction represent the target discharge volumes optimized.

4.4.2 Results Analysis and Discussion

To give a more detail analysis of the trade-offs of four objective, a matrix of scatterplots is shown in Fig. 3. From the plots, a negative correlation can be seen between the upstream flood control objective and downstream flood control objective. The reason is that too much concern about downstream flood control (lower discharge volumes) will lead to a high water level, which may be harmful to upstream flood control. The power generation has a strong correlation with upstream flood control objective. Because higher water level will lead high head, which makes power plant generate more electricity. The navigation rate is weakly related

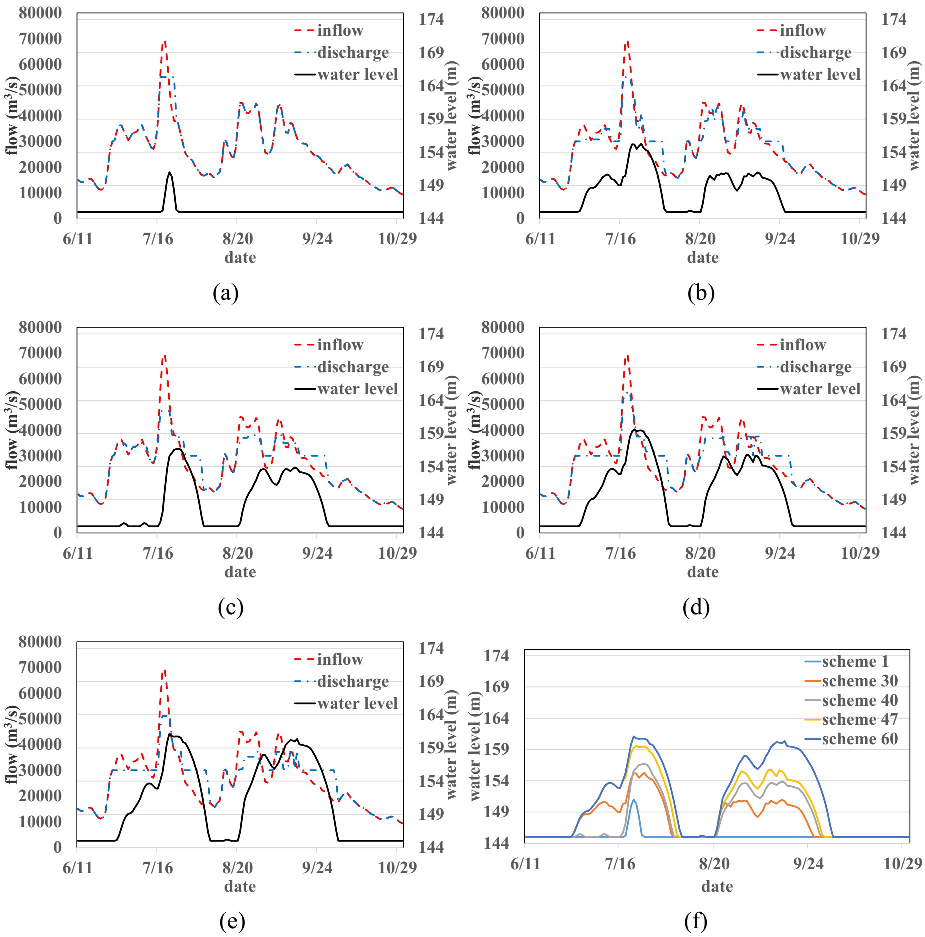

Fig. 5 Discharge processes and water lever processes of **a** Scheme 1, **b** Scheme 30, **c** Scheme 40, **d** Scheme 47, and **e** Scheme 60 for the flood in 1981; **f** water lever process of different schemes for the flood in 1981

to the other three objectives, which means that a scheme with both high navigation rate and high power generation can be found, like Scheme 55.

Two typical years with large floods are chosen from 130 years for the verification. The first year is 1954, which has the largest average inflow 34,000m^3/s during the flood season and its flood peak is 66,100m^3/s, almost a 1% frequency flood. The second year is 1981, which has the largest flood peak 71,100m^3/s and its average inflow is 29,800m^3/s. Figures 4 and 5 shows the water level and discharge processes of five typical schemes with two flood situations. It can be seen from the figures that Scheme 1 minify the discharge to 55,000m^3/s only when the inflow is larger than 55,000m^3/s or the water level is higher than 145 m. This way can maximize the protection of upstream safety, but the power generation will be limited because of the low water level. The 30-th scheme, the 40-th scheme, the 47-th scheme, and the 60-th scheme not only hold back large flood but also hold back small and medium flood that the inflow is less than 55,000m^3/s. In these schemes, more flood resources are used for power generation while the small discharge volume values will helpful for navigation.

5 Conclusions

This paper proposes the HFORs and establishes a mathematical model with four objectives. A novel multi-objective optimization algorithm MOCEA/D is proposed to solve the problem. MOCEA/D combines the advantages of decomposition technology and CA and shows its high performance in some benchmark problems. Then, MOCEA/D is applied to a case study—HFORs for TGP. The experimental results show that MOCEA/D obtains a uniform non-dominated schemes set, which can improve the power generation and navigation rate as much as possible under the premise of ensuring flood control safety.

The HFROs define the current target releases based on the current water level and inflows, it is point out that a reliable inflow forecast can be useful for water recourse management (Liu et al. 2018). Future work includes extending the hierarchical flood operation rule for multi-reservoir systems and considering the inflow forecast to guide the target discharge volume.

Acknowledgements This work is supported by the National Natural Science Foundation of China (No. 91647114, No. 51779013, 51479075), the Natural Science Foundation of Hubei Province (2017CFB613), the Fundamental Research Funds for the Central Universities (HUST: 2016YXZD047), and special thanks are given to the anonymous reviewers and editors for their constructive comments.

Compliance with Ethical Standards

Conflict of Interest The authors declare that they have no conflict of interest.

References

Baltar AM, Fontane DG (2008) Use of Multiobjective Particle Swarm Optimization in Water Resources Management. J Water Resour Plan Manag 134(3):257–265

Chen L, McPhee J, Yeh WWG (2007) A diversified multiobjective GA for optimizing reservoir rule curves. Adv Water Resour 30(5):1082–1093

Coello CAC, Becerra RL (2004) Efficient evolutionary optimization through the use of a cultural algorithm. Eng Optim 36(2):219–236

Cutter SL, Ismail-Zadeh A, Alcántara-Ayala I, Altan O, Baker DN, Briceño S, Gupta H, Holloway A, Johnston D, McBean GA, Ogawa Y, Paton D, Porio E, Silbereisen RK, Takeuchi K, Valsecchi GB, Vogel C, Wu G (2015) Global risks: Pool knowledge to stem losses from disasters. Nature 522(7556):277–279

Das I, Dennis JE (1998) Normal-boundary intersection: A new method for generating the Pareto surface in nonlinear multicriteria optimization problems. SIAM J Optim 8:631–657

Deb K, Pratap A, Agarwal S, Meyarivan T (2002) A fast and elitist multiobjective genetic algorithm: NSGA-II. IEEE Trans Evol Comput 6(2):182–197

Deb K, Thiele L, Laumanns M, Zitzler E (2005) Scalable Test Problems for Evolutionary Multi-Objective Optimization. In: Abraham A, Jain L, Goldberg R (eds) Evolutionary Multiobjective Optimization. Springer-Verlag, London, pp 105–145

Deb K, Jain H (2014) An Evolutionary Many-Objective Optimization Algorithm Using Reference-Point-Based Nondominated Sorting Approach, Part I: Solving Problems With Box Constraints. IEEE Trans Evol Comput 18:577–601

Ding W, Zhang C, Peng Y, Zeng R, Zhou H, Cai X (2015) An analytical framework for flood water conservation considering forecast uncertainty and acceptable risk. Water Resour Res 51(6):4702–4726

Fonseca CM and Fleming PJ (1993) Genetic algorithms for multiobjective optimization: formulation discussion and generalization. In: Forrest S (ed) Proceedings of the Fifth International Conference on Genetic Algorithms, San Mateo, California, pp 416–423. Morgan Kaufmann

Jia B, Simonovic SP, Zhong P, Yu Z (2016) A Multi-Objective Best Compromise Decision Model for Real-Time Flood Mitigation Operations of Multi-Reservoir System. Water Resour Manag 30(10):3363–3387

Karamouz M, Houck MH (1982) Annual and monthly reservoir operating rules generated by deterministic optimization. Water Resour Res 18(5):1337–1344

Landa Becerra R, Coello CAC (2006) Cultured differential evolution for constrained optimization. Comput Method Appl M 195(33–36):4303–4322

Liu Y, Ye L, Qin H, Hong X, Ye J, Yin X (2018) Monthly streamflow forecasting based on hidden Markov model and Gaussian Mixture Regression. J Hydrol 561:146–159

Marien JL, Damázio JM, Costa FS (1994) Building flood control rule curves for multipurpose multireservoir systems using controllability conditions. Water Resour Res 30(4):1135–1144

Needham JT, Watkins DW, Lund JR, Nanda SK (2000) Linear Programming for Flood Control in the Iowa and Des Moines Rivers. J Water Resour Plan Manag 126(3):118–127

Qin H, Zhou J, Lu Y, Li Y, Zhang Y (2010) Multi-objective Cultured Differential Evolution for Generating Optimal Trade-offs in Reservoir Flood Control Operation. Water Resour Manag 24(11):2611–2632

Reddy MJ, Kumar DN (2006) Optimal Reservoir Operation Using Multi-Objective Evolutionary Algorithm. Water Resour Manag 20(6):861–878

Renfrew A. C (1994) “Dynamic Modeling in Archaeology: What, When, and Where?” Dynamical Modeling and the Study of Change in Archaeology, S. E. van der Leeuw, ed., Edinburgh University Press

Reynolds RG (1994) An Introduction to Cultural Algorithms. In: Sebalk AVF (ed) Proceedings of the 3th annual conference on evolution programming. World Scientific, River Edge, pp 131–136

Storn R, Price K (1997) Differential evolution - A simple and efficient heuristic for global optimization over continuous spaces. J Glob Optim 11(4):341–359

Wei C, Hsu N (2009) Optimal tree-based release rules for real-time flood control operations on a multipurpose multireservoir system. J Hydrol 365(3–4):213–224

Yeh WWG (1985) Reservoir Management and Operations Models: A State-of-the-Art Review. Water Resour Res 21(12):1797–1818

Zhang J, Liu P, Wang H, Lei X, Zhou Y (2015) A Bayesian model averaging method for the derivation of reservoir operating rules. J Hydrol 528:276–285

Zhang Q, Li H (2007) MOEA/D: A Multiobjective Evolutionary Algorithm Based on Decomposition. IEEE Trans Evol Comput 11(6):721–731

Zhou Y, Guo S, Xu C, Liu P, Qin H (2015) Deriving joint optimal refill rules for cascade reservoirs with multi-objective evaluation. J Hydrol 524:166–181

Zitzler E, Laumanns M, Thiele L (2001) *SPEA2: improving the strength Pareto evolutionary algorithm*. Paper presented at the Computer Engineering and Networks Laboratory (TIK), Gloriastrasse 35, CH-8092 Zurich, Switzerland